Supporting Information

Takeo et al. 10.1073/pnas.1120367109

SI Methods

Constructs. For creating the pUASp-AttB vector, we amplified a 375-bp fragment containing the attB sequence, which was added with *Aat*II sites at both ends and subcloned into the *Aat*II site of the pUASp vector. The *sra^{WT}-FLAG* construct was made by adding a 3xFLAG tag at the C-terminal end of the *sra* ORF. Briefly, the stop codon of the *sra* gene was replaced with a *Bgl*II site by amplifying *sra* cDNA in pBluescript by PCR using the primers sra-f: 5′-TCATAAGGTGGTGACGAAACT and sra-r: 5′-AGATCTTGCCCGTTCCGGGCACTTGGT. The PCR product was treated with T4 polynucleotide kinase (NEB), self-ligated, and sequenced. A 3xFLAG sequence flanked by BamHI sites was amplified by PCR, digested with BamHI, and inserted into the *Bgl*II site of *sra-Bgl*II cDNA in pBluescript. Point mutations from serine (Ser)/threonine (Thr) to alanine (Ala)/glutamine (Glu)/aspartic acid (Asp) residues were introduced by PCR in the same way as previously described (1). *sra-FLAG* cDNA constructs were cloned into the pUASp-AttB vector. To create the *CnA^{H217Q}* (*CnA^{H217Q}*) transgene, we introduced a single nucleotide substitution of C651 to A into Pp2B-14D ORF (*CnA^{WT}*) in pBluescript using the primers H217Q-f: 5′-GTTGCCGCGCAGCAGGAACA and H217Q-r: 5′-CAAGAGTGCCGGCACTTAACC. The product was treated with T4 polynucleotide kinase, self-ligated, and sequenced. *CnA^{WT}* and *CnA^{H217Q}* constructs were cloned into the pUASp-AttB vector. The ORF region that encodes the major maternal isoform Shaggy (SGG) 10 was amplified by PCR from the *UAS-sgg* line (2) and cloned into the pUASp-AttB vector. The constructs in pUASp-AttB were injected into embryos from the cross of *P{y+.nos-int.NLS}* and *P{CaryP}attP40* transgenes (3–5). After establishing transgenic lines using the second balancer chromosome, the integration between *attP* and *attB* was confirmed by PCR using primers attB-P-f: 5′-GGCTTCACGTTTTCCCAGGTCAGAAGCGGT and attB-P-r: 5′-GCGAATTAGGCCTTCTAGTG.

For creating the *nos-Cre* transgene, which expresses Cre recombinase in germ-line cells, the Cre sequence was cloned into a *P{nosNdeI-nos3′ UTR}* vector [gifted from Satoru Kobayashi (National Institutes of Natural Sciences, Okazaki, Aichi, Japan)]. Transgenic flies were generated by *P* element-mediated transformation.

Preparation of Peptide Mixtures by Triple Digestion. Trichloroacetic acid was added to eluted protein samples at a final concentration of 20% and kept at 4 °C overnight. The samples were centrifuged at 21,920 × *g* for 30 min at 4 °C. The pellet was rinsed with cold acetone two times and solubilized in 60 μL freshly made 0.1 M Tris·HCl, pH 8.5, 8 M urea, and 5 mM Tris(2-carboxylethyl)-phosphine hydrochloride (Pierce). After 30 min of incubation at room temperature, freshly made 0.5 M chloroacetamide (Sigma) was added to a final concentration of 10 mM, and the samples were left at room temperature for another 30 min in the dark. The samples were then split into three aliquots of equal volume (20 μL). For the chymotrypsin (Roche) digestion, urea was diluted to 1.0 M by adding 140 μL 0.1 M Tris·HCl, pH 8.5. Chymotrypsin (0.1 μg) was added to an approximate enzyme to protein ratio of 1:100 (wt/wt) and left to incubate for 6 h at 25 °C. For the Asp-N endopeptidase (Roche) digestion, urea was diluted to 1 M with 0.1 M Tris·HCl, pH 7.8, and Asp-N (1:100 wt/wt) was added for 6 h at 37 °C. For the trypsin digestion, endoproteinase Lys-C (Roche) was first added at 1:100 (wt/wt) enzyme to protein ratio for at least 6 h at 37 °C. Urea was then diluted to 2 M with 0.1 M Tris·HCl, pH 8.5. $CaCl_2$ was added to 0.5 mM, and trypsin (1:100 wt/wt) was added for over 12 h at 37 °C. All enzymatic digestions were quenched by adding formic acid to 5%.

Data Acquisition. Each differently digested sample was analyzed independently by Multidimensional Protein Identification Technology as described previously (6) using a LTQ-Orbitrap hybrid mass spectrometer (Thermo Scientific) interfaced with an Eksigent NanoLC 2D system. The four channels of the nanoLC were filled with 5% acetonitrile, 0.1% formic acid (channels 1A and 2A); 0.5 M ammonium acetate, 5% acetonitrile, 0.1% formic acid (channel 1B); and 80% acetonitrile, 0.1% formic acid (channel 2B). Peptide mixtures were pressure-loaded onto a 100-μm fused silica column pulled to a 5-μm tip using a P-2000 CO_2 laser puller (Sutter Instruments). The microcapillary columns were packed first with 9 cm 5 μm C18 reverse phase (RP) particles (Aqua; Phenomenex) followed by 3 cm 5 μm strong cation exchange material (Partisphere SCX; Whatman) and 1 cm RP particles (7). Loaded microcapillaries were placed in line with the Eksigent NanoLC 2D system and LTQ-Orbitrap hybrid mass spectrometer. Fully automated 10-step chromatography runs were carried out with a flow rate of 500 nL/min measured at 250 nL/min at the tip of the column. Peptides were sequentially eluted from the SCX resin to the RP resin by 10-min-long salt steps of increasing concentrations (0%, 15%, 20%, 30%, 40%, 60%, 70%, 80%, 100%, and 100% for steps 1–10, respectively) followed by the organic gradient to 75% solvent. The application of a 2.5 kV distal voltage electrosprayed the eluting peptides directly into a LTQ-Orbitrap hybrid mass spectrometer equipped with a nano-LC electrospray ionization source (Thermo Scientific). Full MS spectra were recorded on the peptides over a 400–1,600 *m/z* range in the Orbitrap at 60 K resolution followed by fragmentation in the ion trap (at 35% collision energy) on the first to fifth most intense ions selected from the full MS spectrum. Dynamic exclusion was enabled for 120 s (8), with an exclusion window of 0.03–1.03. Mass spectrometer scan functions and HPLC solvent gradients were controlled by the Xcalibur data system (Thermo Scientific).

Data Analysis. RAW files were extracted into ms2 file format (9) using RawDistiller (REF) (10). First, MS/MS spectra were searched using SEQUEST (11) with a peptide mass tolerance of 20 ppm and without specifying differential modifications against a protein database consisting of 18,323 *Drosophila* proteins (downloaded from the National Center for Biotechnology Information on December 23, 2009) as well as 177 usual contaminants such as human keratins, IgGs, and proteolytic enzymes. To estimate false discovery rates (FDR), each protein sequence was randomized (keeping the same amino acid composition and length), and the resulting shuffled sequences were added to the database used for the SEQUEST searches. To account for alkylation by chloroacetamide (CAM), +57 Da were added statically to cysteine residues for all searches.

Second, the same ms2 files were also searched for posttranslational modifications against a database containing only the sequences for the proteins of interest [i.e., Sarah CG6072-PA (Sra), Calcineurin B2 CG11217-PA (CanB2), Protein phosphatase 2B at 14D CG9842-PA (Pp2B-14D), Calmodulin CG8472-PB, isoform B and Calcineurin A at 14F CG9819-PB, isoform B (CanA-14F), and Sra^{S215A}] using SEQUEST (11) with a peptide mass tolerance of 7 ppm. As described in ref. 12, phosphorylation modification searches were set up for peptides containing phosphorylated threonines, Sers, and tyrosines (+79.9663). The maximum number of modified amino acids per differential modi-

fication in a peptide was limited to four. After this round of searches, an in-house developed script, sqt-merge (13), was used to combine the two sets of SEQUEST output files (sqt files) generated from the normal search (i.e., without modifications) and posttranslational modifications searches described above into one set. The sqt-merge script read in sqt files from normal and differentially modified searches generated from the same ms2 files and then merged and ranked the spectrum/peptide matches based on cross-correlation scores (XCorrs). Normalized differences in XCorrs (DeltCn) values were recalculated. This merging step allowed only the best matches out of *n* differential SEQUEST queries to be ranked first.

Third, only spectra passing conservative filtering criteria (DeltCn of at least 0.05, minimum XCorr of 1.8 for +1, 2.0 for +2, and 3.0 for +3 spectra, maximum Sp rank of 10, and minimum peptide length of 7 aa) and matching modified peptides were selected (−m 0 −t 0 DTASelect parameters), and their coordinates written out into smaller ms2 files using the copy utility of DTASelect (14). These subsetted ms2 files contained, at best, a few hundred MS/MS spectra and were subjected to the same differential modification searches against the complete database described above (including shuffled sequences). Again, sqt-merge was used to bring together the results generated by these different searches. This step allowed us to check that spectra matching modified peptides from protein sequences of interest did not find a better match against the larger protein database. All spectra matching modified peptides were visually assessed and given an evaluation flag (yes/maybe/no). The no matches were removed from the final data (−v 2 parameter in DTASelect). Spectra/peptide matches were only retained if they had a DeltCn of at least 0.08 and minimum XCorr of 1.8 for singly charged, 2.5 for doubly charged, and 3.5 for triply charged spectra. In addition, the peptides had to comply with the enzyme specificities (Typsin: preceding and last amino acids were arginines or lysines; Chymotrypsin: preceding and last amino acids were phenyalanine, tryptophan, tyrosine, or leucine; Asp-N endopeptidase: first and immediate following amino acids were aspartic acid or glutamate) and be at least 7 aa long. DTASelect (14) was used to select and sort peptide/spectrum matches passing these criteria. U_SPC6 software [in house software by Tim Wen (Stowers Institute for Medical Research, Kansas City, MO)] was used to extract total and modified spectral counts for each amino acid of the proteins of interest and calculate modification levels based on local spectral counts (15). *NSAF7* (Tim Wen) was used to create a final report on all detected proteins across the different runs, calculate their respective distributed normalized spectral abundance factor (dNSAF) values, and FDRs (16–18) (Eq. **S1**):

$$FDR = \frac{2 \times SHUFFLED\_SpectralCounts}{Total\_SpectralCounts} \times 100 \text{ and} \qquad \textbf{[S1]}$$

(Eq. **S2**)

$$(NSAF)_i = \frac{(SpectralCount/Length)_i}{\sum_{k=1}^{N} (SpectralCount/Length)_k}. \qquad \textbf{[S2]}$$

Under these criteria, the overall FDR at the spectral level was less than 1%. To estimate relative protein levels for Sra and calcinuerin proteins, dNSAFs were calculated for Sra, CanB2, Pp2B-14D, Calmodulin, CanA-14F, and Sra^{S215A}, and they are presented in Fig. S5*B*. In addition, a Power Law Global Error Model was applied to the entire dataset to determine differentially abundant proteins when two biological conditions were compared (19).

1. Takeo S, Hawley RS, Aigaki T (2010) Calcineurin and its regulation by Sra/RCAN is required for completion of meiosis in *Drosophila*. *Dev Biol* 344:957–967.
2. Bourouis M (2002) Targeted increase in shaggy activity levels blocks wingless signaling. *Genesis* 34:99–102.
3. Bischof J, Maeda RK, Hediger M, Karch F, Basler K (2007) An optimized transgenesis system for *Drosophila* using germ-line-specific phiC31 integrases. *Proc Natl Acad Sci USA* 104:3312–3317.
4. Fish MP, Groth AC, Calos MP, Nusse R (2007) Creating transgenic *Drosophila* by microinjecting the site-specific phiC31 integrase mRNA and a transgene-containing donor plasmid. *Nat Protoc* 2:2325–2331.
5. Markstein M, Pitsouli C, Villalta C, Celniker SE, Perrimon N (2008) Exploiting position effects and the gypsy retrovirus insulator to engineer precisely expressed transgenes. *Nat Genet* 40:476–483.
6. Washburn MP, Wolters D, Yates JR, 3rd (2001) Large-scale analysis of the yeast proteome by multidimensional protein identification technology. *Nat Biotechnol* 19: 242–247.
7. McDonald WH, Ohi R, Miyamoto DT, Mitchison TJ, Yates JR (2002) Comparison of three directly coupled HPLC MS/MS strategies for identification of proteins from complex mixtures: Single-dimension LCMS/MS, 2-phase MudPIT, and 3-phase MudPIT. *Int J Mass Spectrom* 219:245–251.
8. Zhang Y, Wen Z, Washburn MP, Florens L (2009) Effect of dynamic exclusion duration on spectral count based quantitative proteomics. *Anal Chem* 81:6317–6326.
9. McDonald WH, et al. (2004) MS1, MS2, and SQT-three unified, compact, and easily parsed file formats for the storage of shotgun proteomic spectra and identifications. *Rapid Commun Mass Spectrom* 18:2162–2168.
10. Zhang Y, Wen Z, Washburn MP, Florens L (2011) Improving proteomics mass accuracy by dynamic offline lock mass. *Anal Chem* 83:9344–9351.
11. Eng JK, McCormack AL, Yates JR, III (1994) An approach to correlate tandem mass spectral data of peptides with amino acid sequences in a protein database. *J Am Soc Mass Spectrom* 5:976–989.
12. Mohan M, et al. (2010) Linking H3K79 trimethylation to Wnt signaling through a novel Dot1-containing complex (DotCom). *Genes Dev* 24:574–589.
13. Zybailov B, Coleman MK, Florens L, Washburn MP (2005) Correlation of relative abundance ratios derived from peptide ion chromatograms and spectrum counting for quantitative proteomic analysis using stable isotope labeling. *Anal Chem* 77: 6218–6224.
14. Tabb DL, McDonald WH, Yates JR, 3rd (2002) DTASelect and Contrast: Tools for assembling and comparing protein identifications from shotgun proteomics. *J Proteome Res* 1:21–26.
15. Xiang Y, et al. (2007) The inhibition of polo kinase by matrimony maintains G2 arrest in the meiotic cell cycle. *PLoS Biol* 5:e323.
16. Florens L, et al. (2006) Analyzing chromatin remodeling complexes using shotgun proteomics and normalized spectral abundance factors. *Methods* 40:303–311.
17. Paoletti AC, et al. (2006) Quantitative proteomic analysis of distinct mammalian Mediator complexes using normalized spectral abundance factors. *Proc Natl Acad Sci USA* 103:18928–18933.
18. Zybailov B, et al. (2006) Statistical analysis of membrane proteome expression changes in Saccharomyces cerevisiae. *J Proteome Res* 5:2339–2347.
19. Pavelka N, et al. (2008) Statistical similarities between transcriptomics and quantitative shotgun proteomics data. *Mol Cell Proteomics* 7:631–644.

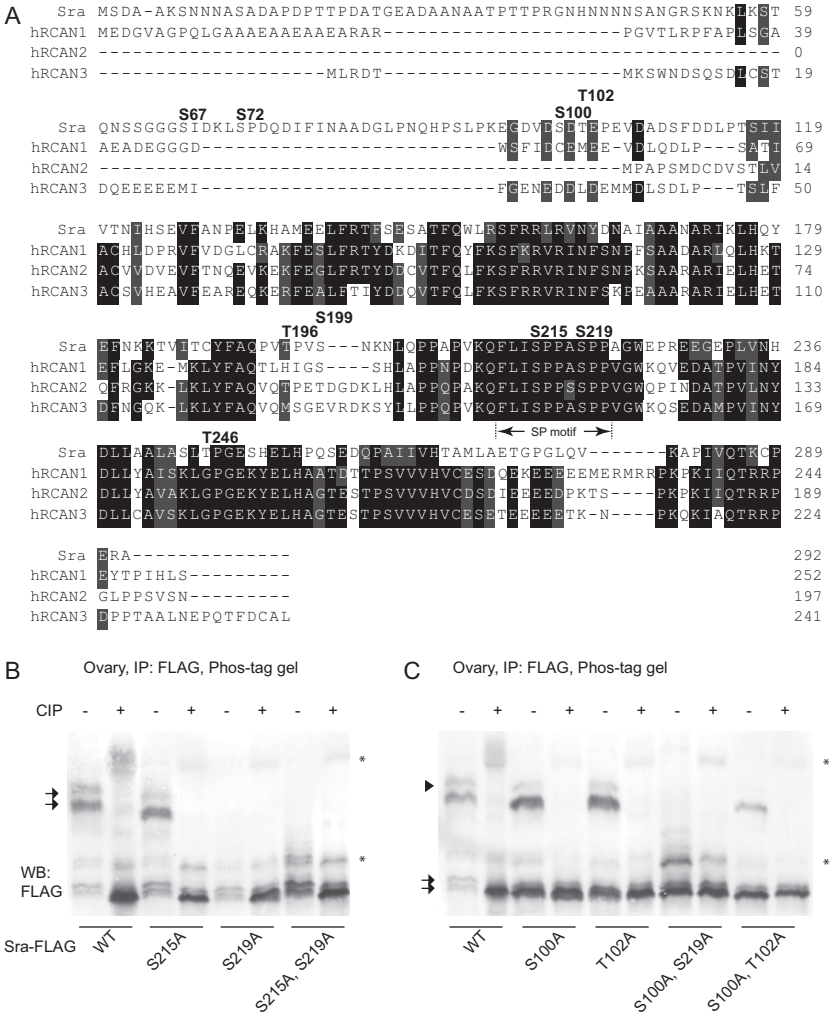

Fig. S1. Analyses of Sra phosphorylation sites. (*A*) Alignment of amino acid sequences between Sra and human regulators of calcineurin. The residues that are identical (black) or similar (gray) among three or more sequences are boxed. The positions of identified Ser/Thr residues and Ser199 of Sra are shown above the sequence. (*B* and *C*) Western blot analysis of Sra-FLAG proteins. Ovary extracts overexpressing WT Sra-FLAG and Sra^{mut}-FLAG were immunoprecipitated with FLAG affinity beads and analyzed by phosphate binding tag (Phos-tag)/Western blot. Asterisks indicate nonspecific signals. The slower bands (arrows in *B*) in WT without calf intestinal alkaline phosphatase treatment are absent when Ser219 is mutated to Ala, suggesting that these forms include phosphorylation at least at Ser219. The fastest doublet bands (arrows in *C*) in WT without calf intestinal alkaline phosphatase treatment are absent when Ser100 or Thr102 is mutated to Ala, and the slowest band (arrowhead in *C*) is absent in the Ser100/Thr102 double mutant.

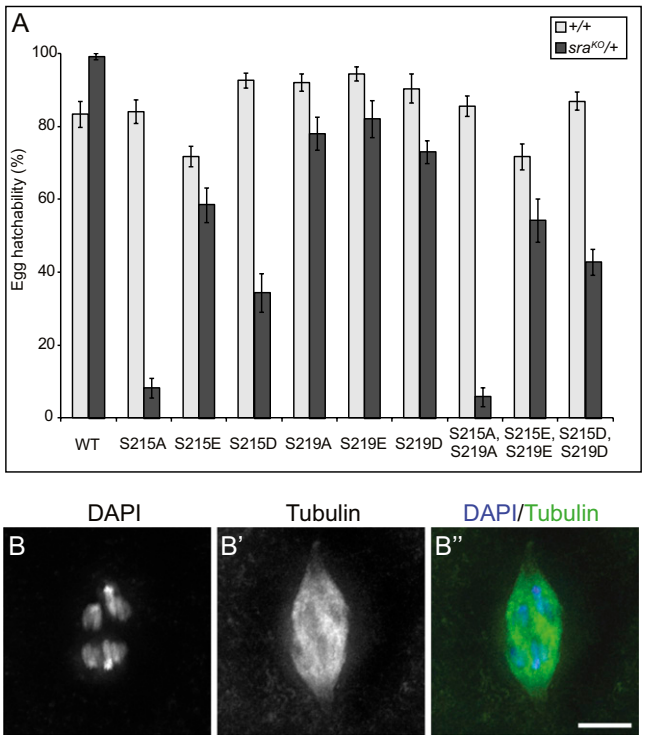

Fig. S2. Genetic analyses of Ser215 and Ser219. (*A*) The hatch rate of eggs from females that express Sra^{WT} (WT) or mutant forms of Sra with the substitution at Ser215, Ser219, or both in WT (light gray bars) or heterozygous (dark gray bars) sra^{KO} background was tested. Error bars indicate 95% confidence intervals. (*B*) A typical meiotic defect in *nos* > sra^{S215A}*-FLAG;* sra^{KO}/+ eggs. Chromosomes (*B*) and spindles (*B′*) are stained with DAPI and anti-α-tubulin antibody, respectively, and the merged images are shown in *B″*. (Scale bar: 5 μm.)

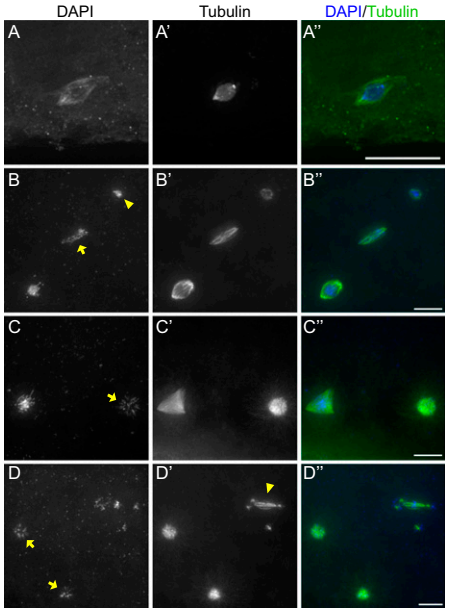

Fig. S3. sgg^{D127} eggs fail to complete meiosis properly. (*A*) Metaphase I arrest was normal in mature oocytes from sgg^{D127} germ-line clones. (*B–D*) Among the 70.8% of sgg^{D127} eggs that failed to complete meiosis normally, there were multiple (two to four) signals that were stained with DAPI and anti–α-tubulin in the 62.5% of cases. The configuration of chromosomes and spindles in these eggs was variable among eggs, but a large number of DAPI signals contained thread-like (arrow in *B*), overcondensed (arrowhead in *B*), or rosette-like (arrow in *C*) chromosomes in spindles of abnormal size and shape. The remaining 8.3% of eggs seemed to have multiple polar body rosettes (arrows in *D*) and an abnormally shaped spindle that appeared to be at the first mitotic division (arrowhead in *D′*). Therefore, it is likely that these eggs are able to arrest and reinitiate meiosis but fail to divide chromosomes properly at meiosis II or fail to form a polar body rosette and pronucleus. Chromosomes (*A–D*) and spindles (*A′–D′*) are stained with DAPI and anti-α-tubulin antibody, respectively, and the merged images are shown in *A″–D″*. (Scale bars: 10 μm.)

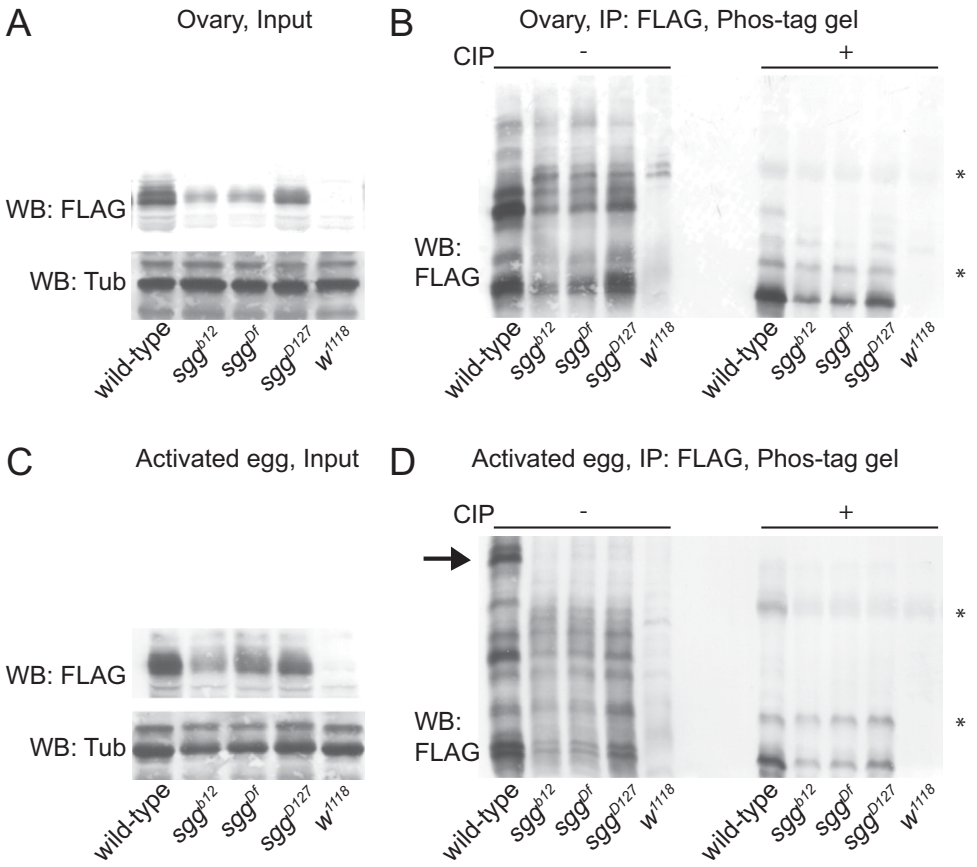

Fig. S4. Sra phosphorylation at Ser215 is absent in *sgg* mutant eggs. Western blot analyses of Sra-FLAG in WT and *sgg* mutant ovaries (*A* and *B*) and activated eggs (*C* and *D*). w^{1118} was used as a negative control. Equal volumes of samples were analyzed by Western blot with anti-FLAG and anti–α-tubulin (for loading control) antibodies (*A* and *C*). Note that the abundance of Sra-FLAG on the control lane is higher than the abundance in *sgg* mutants, suggesting that the stability of Sra is affected in *sgg* mutants. Protein lysates were immunoprecipitated with FLAG beads, and phosphorylation of Sra-FLAG was analyzed by phosphate binding tag (Phos-tag)/Western blot (*B* and *D*). Asterisks indicate nonspecific signals (details in Fig. 2). Although the pattern of Sra-FLAG bands does not differ between the WT and *sgg* mutants in the ovary, the signal that represents phosphorylation at Ser215 (arrow) is absent in activated eggs from *sgg* mutants (Fig. 3*F*). CIP, calf intestinal alkaline phosphatase.

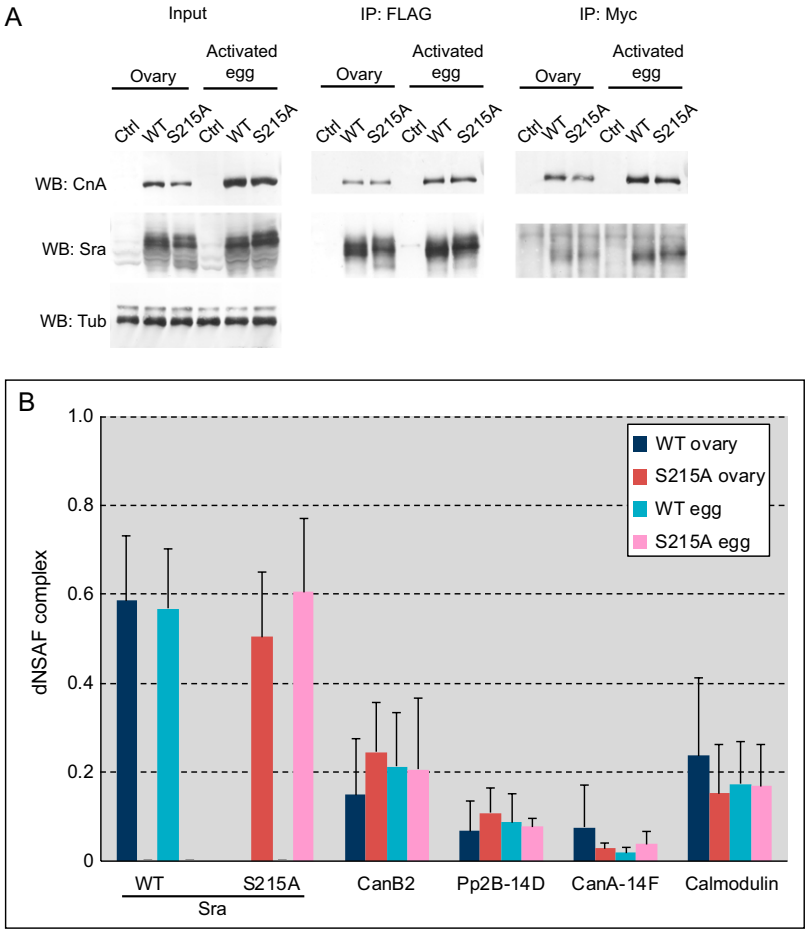

Fig. S5. Sra is not dissociated from calcineurin on egg activation. (*A*) Ovaries or activated eggs from females expressing CnA-Myc and Sra-FLAG were tested. w^{1118} was used as a negative control (Ctrl). Reciprocal coimmunoprecipitation was performed with anti-FLAG and anti-Myc antibodies. Sra is associated with calcineurin in both ovaries and activated eggs, and a mutation at Ser215 does not affect the level of interaction between Sra and CnA. (*B*) Relative abundance of Sra, calcineurin proteins, and Calmodulin in ovaries and activated eggs. The average of dNSAF values of proteins of interest was calculated from at least four independent Multidimensional Protein Identification Technology datasets for each biological sample. Error bars indicate SD.